

Identification of Key Genes and Pathways Associated with Mast Cells Resting in Meningioma

Hui Xie

Shenyang Medical College

Xiao-hui Ding

Shenyang Medical College

Ce Yuan

University of Minnesota

Jin-jiang Li

General Hospital of Northern Theater Command

Zhao-yang Li

China Medical University

Wei-cheng Lu (✉ 87k10b@163.com)

First Affiliated Hospital of China Medical University <https://orcid.org/0000-0002-8127-6628>

Primary research

Keywords: meningioma, mast cells resting, differentially expressed genes, pathways, miRNAs

Posted Date: September 24th, 2020

DOI: <https://doi.org/10.21203/rs.3.rs-80140/v1>

License:  This work is licensed under a Creative Commons Attribution 4.0 International License.

[Read Full License](#)

Abstract

Background: To identify candidate key genes and pathways related to mast cells resting in meningioma and the underlying molecular mechanisms of meningioma.

Methods: Gene expression profiles of GSE43290 and GSE16581 datasets were obtained from the Gene Expression Omnibus (GEO) database. GO and KEGG pathway enrichments of DEGs were analyzed using the ClusterProfiler package in R. The protein-protein interaction network (PPI), and TF-miRNA- mRNA co-expression networks were constructed. Further, the difference in immune infiltration was investigated using the CIBERSORT algorithm.

Results: A total of 1499 DEGs were identified between tumor and normal controls. The analysis of the immune cell infiltration landscape showed that the probability of distribution of memory B cells, regulatory T cells (Tregs), and resting mast cells in tumor samples were significantly higher than those in the controls. Moreover, through WGCNA analysis, the module related to mast cells resting contained 158 DEGs, and KEGG pathway analysis revealed that the DEGs were dominant in the TNF signaling pathway, cytokine-cytokine receptor interaction, and IL-17 signaling pathway. Survival analysis of hub genes related to mast cells resting showed that the risk model was constructed based on 9 key genes. The TF-miRNA- mRNA co-regulation network, including MYC-miR-145-5p, TNFAIP3-miR-29c-3p, and TNFAIP3-hsa-miR-335-3p, were obtained. Further, 36 nodes and 197 interactions in the PPI network were identified.

Conclusions: The results of this study revealed candidate key genes, miRNAs, and pathways related to mast cells resting involved in meningioma development, providing potential therapeutic targets for meningioma treatment.

Background

Meningioma, originating from meningotheelial cells, is the most common primary brain tumor, accounting for 35–40% of central nervous system (CNS) tumors, with an incidence of approximately 2 in 100,000 adults [1, 2]. There is an about 3:1 female predominance of meningioma due to the role of estrogen [3, 4]. Meningioma is often associated with headaches, imbalances, impaired vision, and other neurological problems that can leave the patient very weak [5]. According to the WHO's classification of nervous tissue tumors, meningiomas belong to the meningotheelial-cell tumors of the meninges, and are classified into grades I, II and III. Treatment for meningioma encasing crucial neural and vascular structures, and for more aggressive histological types such as anaplastic (grade III), may be very challenging. Although most meningioma are classified as WHO grade I (85–95%), and considered as benign solid tumors, the tumors can recur even after complete resection, and the recurrence rate in these patients have been reported to be 7.5% or 9.3% in 10 and 20 years, respectively [6, 7]. It is therefore of great value to explore the molecular mechanism underlying the development of meningioma, as it will aid in disease treatment and patient prognosis improvement.

Generally, the development and growth of a tumor usually requires the appropriate microenvironment, as well as genetic/molecular changes in the tumor cell. An increasing number of evidence reports that the malignant phenotype of tumor is influenced by the tumor-related microenvironment [8–10]. The tumor-related microenvironment consists of tumor immune cell types, density, and localization, and accumulating evidence has shown correlations between immune cell infiltration in different human tumors and clinical outcomes [11, 12]. Meningioma, an immune-sensitive malignant tumor, is infiltrated by numerous immune cells, including CD8 lymphocytes, macrophages and mast cells (MCs) [13]. In different types of meningiomas, a variety of phenotypes of MCs are found primarily in the lobule of connective tissues, including malignancies independent of growth rate, grade, or degree of calcification. In the last several decades, the importance of mast cells under several physiological and pathological conditions, has been described. However, their molecular mechanism in meningioma development remains unknown [14]. In the present study, we retrieved the meningioma-associated microarray data from Gene Expression Omnibus (GEO) databases in order to investigate tumor immune cell-related genes, transcription factors (TF), functional processes, and pathways that could be significantly correlated with meningioma development and overall patient survival. Further analysis performed included tumor-immune cell related Differentially Expressed Gene (DEG) screening, Gene Ontology (GO), Kyoto Encyclopedia of Genes and Genomes (KEGG) enrichment analysis, survival analysis, TF-miRNA- mRNA and TF-miRNA- mRNA construction, Protein-Protein Interaction (PPI), and drug-gene construction.

Materials And Methods

Data source

In this study, the GSE43290 dataset containing the gene expression profiles from meningioma tumor tissues obtained from 47 patients and 4 normal control samples, was downloaded from the Gene Expression Omnibus (GEO) database (GSE43290: updated August 10, 2018; <https://www.ncbi.nlm.nih.gov/geo/>) and accessed with GPL96 [HG-U133A] Affymetrix Human Genome U133A Array platform. GSE77259 dataset, which contained 17 samples (14 meningioma tumor tissues samples and 3 normal samples) was selected as the validation data, and assessed by the platform of [HuGene-1_0-st] Affymetrix Human Gene 1.0 ST Array. For survival analysis, the GSE16581 dataset (updated May 25, 2019) including the overall-survival (OS) data for 68 meningioma patients was accessed using the GPL570 [HG-U133_Plus_2] Affymetrix Human Genome U133 Plus 2.0 Array platform.

Data preprocessing and identification of DEGs

According to the Series Matrix data Files of GSE43290, GSE77259 and GSE16581, each dataset was normalized independently using Robust Multiarray Average (RMA) algorithm in the Affy Bioconductor package in R [15, 16]. The Bioconductor annotation packages for GSE43290 and GSE16581 were specifically hgu133a.db, hugene10sttranscriptcluster.db and hgu133plus2.db. Afterwards, the FactoMineR package in R was used for principal component analysis (PCA) and clustering.

To identify the DEGs between meningioma and normal samples, the improved t-test method based on empirical bayes provided by the limma R package (Version: 3.40.6) [17] was used with the threshold of P-value<0.05 and $|logFC|>1$. Volcano Plot of DEGs was obtained through the ggpubr package in R (version 0.2.2), and hierarchical clustering was performed using pheatmap package in R ($|logFC|>2$). Principal Component Analysis (PCA) and clustering analysis for the DEG were conducted using the FactoMineR package in R with $|logFC| > 2$.

Analysis of Abundance of infiltrating immune cells

The CIBERSORT deconvolution algorithm [18] was used to estimate the matrix of abundant immune cells on the expression matrix of the samples, so as to analyze the abundance of infiltrating immune cells. The parameters were set as perm=100 and QN=TRUE. The barplot, pheatmap and vioplot were plotted using R language. $P < 0.05$ was considered as subsets of immune cells with significant differences.

Screening immune cell related modules and genes

Based on tumor samples of immune maceration, the DEGs were analyzed by using the WGCNA package in R software (Version 1.68) [19]. The gene sets that significantly correlated with the degree of infiltration of different immune cell subsets were screened, and the genes were found to be related to the immune cell subsets. The boxplot of immune-related DEGs between tumor and normal samples was constructed based on the ggboxplot function of ggpubr package in R.

Survival analysis

Survival analysis was performed using Survival package (version 2.44-1.1) with log rank test (cut off: P.value<0.05) was used based on the immune-related DEGs and clinical information of GSE16581, and survival curve was constructed. Univariate and multivariate Cox regression analysis was conducted using the coxph method in survival package [20], and ggforest package in R was used for HR forest mapping construction.

Construction of TF-miRNA- mRNA co-expression network

miRWalk3.0, miRDB, TargetScan, and miRTarBase were used to predict miRNA-mRNA interactions. TF-mRNA pairs were obtained using the online database TRRUST (<https://www.grnpedia.org/trrust/>) [21]. The co-expression network was constructed using Cytoscape software, and enrichment analysis was carried out for transcription factors of DEGs in the risk model.

Functional enrichment analysis

For the functional annotation of DEGs, the ClusterProfiler package in R (Version 3.12.0) was used to identify the enriched GO terms and KEGG pathways. The results were considered to be significant with FDR adjusted $p < 0.05$.

Screening of pathways associated with meningioma

Out of the pathways associated with meningioma in CTD $\text{\texttt{http://ctdbase.org/}}$, KEGG pathway enriched by transcription factors and immune-related genes was further screened, and a pathway diagram drawn with the pathview package in R (version 1.24.0).

Protein-protein interaction (PPI) network construction

In order to further predict the interaction of protein pairs, the Search Tool for the Retrieval of Interacting Genes (STRING) database [22] was used with a confidence score > 0.7 . And the PPI integrated networks were mapped by Cytoscape 3.4.0 software [23]. Finally, MCODE [24] was used to screen the modules of hub genes from the PPI network, with the node Score ≥ 10 as cut-off criterion.

The prediction of drug-gene interaction

Drug-gene interaction was predicted by Drug Gene Interaction database (DGIdb) 3.0 (Version: 3.0.2) [25], and the network was constructed with the Cytoscape software. The DrugBank database [26] was used to retrieve information about predicted drugs.

Results

Identification of DEGs

Following differential gene expression analysis and filtering with the cut-off criteria of P . value < 0.05 & $|logFC| > 1$, the DEGs between tumor and normal cells were screened. For the GSE43290 dataset, a total of 1499 DEGs were identified, out of which 73 were up-regulated and 1426 were down-regulated. For the GSE77259 dataset, 4830 DEGs, including 2536 up-regulated and 2294 down-regulated genes, were identified. Moreover, a total of 673 overlapping DEGs, such as *MYC*, *TNFAIP3* and *SLC2A3* in both GSE43290 dataset and validation GSE77259 dataset were obtained (Supplementary figure 1).

Furthermore, volcano plot and PCA clustering of DEGs in GSE43290 showed that the differentially expressed DEGs between the two groups could be significantly distinguished (Figure 1A and 1B).

Furthermore, using a threshold of $|logFC| > 2$, 255 DEGs were analyzed using the bilayer cluster analysis (Figure 1C) to further predict the potential functions of the dysregulated mRNAs in meningioma, detected by enrichment analysis. The results of GO analysis showed that these enriched mRNAs were functionally classified by Biological Process (BP), Cellular Component (CC), and Molecular Function (MF) (Figure 1D). Among them, several BPs seemed to be related to the mechanisms of HF; moreover, CCs and MFs were found to be mainly associated with regulation of cardiac electrical activity. Furthermore, KEGG pathway analysis revealed a series of enriched pathways, such as IL-17 signaling pathway and TNF signaling pathway (Figure 1E)

The immune cell infiltration landscape

Based on the gene expression profiles of GSE43290, the difference in immune infiltration between tumor and control samples among 22 immune cells types, were detected using CIBERSORT algorithm. As shown in Figure 2A, 48 of the 51 samples were valid (P value <0.05), including 44 tumor samples and 4 normal samples. Among the 22 immune cell types, the percentage of CD8+ T cells (yellow) and M2 macrophages (blue) in each sample was relatively high. The heatmap showing the 22 tumor immune cells was illustrated in Figure 2B. Based on the violin plot (Figure 2C), the probability of distribution of memory B cells, regulatory T cells (Tregs) and resting mast cells in tumor were obviously higher than those in the control samples (all, $P<0.05$), indicating that the immune infiltration proportions could be useful in distinguishing meningioma patients from healthy patients.

In addition, a lot of literature have shown that mast cells (MC) were associated with the development of meningioma [13, 14, 27], and resting mass cells infiltration ratio was relatively high in this study. Hence, the follow-up analysis focused on resting mast cells.

Weighted correlation network analysis (WGCNA) co-expression networks

When correlation coefficient threshold was set at 0.85, the soft-thresholding power was 6 (Supplementary figure 2A). Through WGCNA analysis, 10 co-expression modules were constructed based on the 1499 DEGs (Supplementary figure 2B), of which the grey module was the gene set that could not gather into other modules, so there were only 9 valid gene modules.

Subsequently, as shown in Figure 3C, the correlation between each module and the degree of invasion of immune cells in tumor tissue was calculated. The results revealed that yellow, the module with the highest correlation, contained 158 DEGs, consisting of 2 up-regulated and 156 down-regulated genes (Supplementary table 1). Yellow modules are negatively related to degree of resting mast cells infiltration in meningioma tissues, and the correlation between genes in the yellow module and the degree of immune cell infiltration was summarized in the Supplementary table 2.

Furthermore, GO functional analysis revealed that the genes in yellow module were dominant in biological processes involved in response to leukocyte migration, molecules of bacterial origin, and inflammatory response (Figure 4A); KEGG pathway analysis revealed that the genes were mainly enriched in the TNF signaling pathway, cytokine-cytokine receptor interaction and IL-17 signaling pathway (Figure 4B). The path diagram was annotated based on the pathview package in R, (Figure 4C).

Risk model construction of key genes

In order to identify whether each key gene related to mast cells resting correlated with prognosis of meningioma patients, univariate and multivariate analyses were performed. K-M survival analysis revealed that *CXCL8* and *MYC* were associated with prognosis of meningioma patients. Moreover, based on the COX univariate and multivariate regression analyses showed *CXCL8* and *MYC* might be prognostic biomarkers for meningioma patients (Table 1 and 5A).

Subsequently, based on the 9 genes in univariate regression analysis above, the risk model was constructed. Firstly, the meningioma patients were categorized into low- or high-risk patients, and the cut off value was the median risk score (Figure 5B). The scatter plot of survival time of risk model samples showed that the survival time of samples was relatively lower in the high-risk group than the low-risk group (Figure 5C). Monolayer clustering analysis of RNA expression in the risk model of each sample showed differences in the key genes between high and low risk groups (Figure 5D). Moreover, K-M survival curve indicated that the survival time between the high and low risk groups was significantly different (P value = 0.00436; Figure 5E), suggesting the risk model of 9 key gene related to mast cells resting was successfully constructed.

TF-miRNA- mRNA co-regulation network

Based on the database (miRWalk3.0, TargetScan, MiRDB, and MirTarBase) with the Score > 0.95, 145 miRNAs acting on 3'UTR region of the genes in the risk model associated with mast cells-resting immune cells were predicted. Then, according to the retrieval of HMDD V3.2 database, 3 miRNA-mRNA pairs (including MYC-miR-145-5p, TNFAIP3-miR-29c-3p and TNFAIP3-miR-335-3p) were obtained, respectively. Subsequently, and 37 TF-mRNA pairs (including 6 mRNAs and 27 TFs) were screened using the online database of TRRUST. Lastly, based on mRNA-miRNA pairs and TF-mRNA pairs, miRNA-TF-mRNA co-regulation network (ceRNA) was constructed using Cytoscape (Figure 6A).

Additionally, in order to further investigate the potential biological functions of the genes involved in ceRNA network, the GO terms and KEGG pathway analyses were conducted. As illustrated in Figure 6B, the functional processes of the genes were primarily related to biological regulation, while KEGG pathway analysis revealed that the genes were enriched in Tumor Necrosis Factor (TNF) signaling pathway and IL-17 signaling pathway (Figure 6C).

PPI network and modules analysis

According to STRING database, the PPI network (PPI score = 0.4) was constructed with 27 TFs in miRNA-TF-mRNA co-regulation network and 9 DEGs in the risk model using Cytoscape. As shown in Figure 7A, there were 36 nodes and 197 interactions in the PPI network. With score > 12, a module with 15 nodes and 88 interactions was further revealed from the PPI network using the MCODE of Cytoscape software (Figure 7B).

Drug-gene network

Similarly, based on the 9 DEGs in the risk model, a total of 50 drug-gene interacting pairs, including 3 target genes (*CXCL2*, *CXCL8* and *MYC*), and 49 drugs were identified using the DGIdb 3.0 database. Furthermore, drug-gene interaction network was constructed by Cytoscape software (Figure 8).

Discussion

Till now, the etiology of meningioma has not been fully elucidated, however, it is believed to involve environmental and genetic factors, with genetic factors being the important factors determining its development. Hence, in the present study, according to the microarray data from GEO database, we screened a series of genes, including *MYC* and *CXCL8*, as well as the TNF signaling pathway, cytokine-cytokine receptor interaction, and IL-17 signaling pathway, related to mast cells resting which are involved meningioma pathogenesis and prognosis. Moreover, based on the 9 key genes related to mast cells resting in meningioma, the PPI network, TF-miRNA- mRNA network, drug-gene interaction network were constructed, respectively; among which, the key miRNAs and TF that might play important roles in meningioma were selected.

Tumor immunotherapy has achieved promising results in clinical application [28, 29]. To identify new indicators for meningioma prognosis improvement, an increasing number of reports have focused on tumor-infiltrating immune cells, in accordance with the function and composition of tumor cells in cancer occurrence and development [13, 14, 30–32]. In our study, based on the analysis of abundant infiltrating immune cells (CIBERSORT deconvolution algorithm with the parameters of perm = 100 and QN = TRUE), we found that the probability of distribution of memory B cells, regulatory T cells (Tregs) and resting mast cells in tumor samples was significantly higher than that in control samples. Actually, although some literature showed that T cells regulatory cells (Tregs) associated with Meningioma [30–32], our subsequent analysis of T cell regulation did not turn out well. In addition, there is increasing underlying evidence of the association between mast cells and meningioma development [13, 14, 33], but the molecular mechanism of mast cells in meningioma immunotherapy remains unclear.

In order to explore the genes related to infiltration of mast cells resting in meningioma tissue, WGCNA analysis with R language package was performed on DEGs of meningioma patients and normal controls. The results showed yellow modules are negatively related to the degree of infiltration of resting mast cells in meningioma tissues, thus, genes such as *MYC*, *CXCL2*, *CXCL8* and *FOSL1* in the module, are inversely associated with the degree of mast cell infiltration. Pathway analysis revealed that the genes were mainly enriched in the TNF signaling pathway, cytokine-cytokine receptor interaction, and IL-17 signaling pathway. It has been reported that the cytokine-cytokine receptor interaction signaling pathway is involved in the meningioma. Additionally, although the TNF signaling pathway or IL-17 signaling pathway is rarely studied in meningioma, many researches have revealed the activation of the TNF or IL-17 signaling pathway in various brain diseases such as neuroinflammatory injury [34], autoimmune encephalomyelitis [35], and ischemic stroke [36]. Moreover, survival analysis (Survival package with log-rank test; threshold value of P value < 0.05) of key genes related to resting mast cells showed that the risk model constructed based on 9 key genes (*CXCL8*, *MYC*, *CXCL2*, *CXCL3*, *TNFAIP3*, *FOSL1*, *HIST1H2BN*, *BCL2A1* and *SLC2A3*) could predict the prognosis of patients with meningioma. A previous study reported that *MYC* expression is dysregulated in human meningioma, indicating its potential role in oncogenic processes [37]. Cai et al [38] found that c-MYC in meningioma is targeted by RIZ1 to negatively regulate the ubiquitin-binding enzyme E2C/UbcH1. It has also been found that the methylation of Werner syndrome protein is associated with invasive meningioma occurrence and development via *MYC* expression regulation [39]. More importantly, *MYC* is associated with the TNF signaling and cytokine-

cytokine receptor interaction pathways. Similarly, it has been found that CXC receptor activates ERK1/2 and stimulates meningioma cell proliferation [40], and in systematic investigation of quercetin for cardiovascular disease treatment, CXCL8 is enriched in the TNF signaling and IL-17 signaling pathways [41]. Hence, we speculate that the key genes, including *MYC* and *CXCL8*, are involved in meningioma progression via the regulating of different pathways such as the TNF signaling pathway, cytokine-cytokine receptor interaction, and IL-17 signaling pathway.

With the increasing studies on miRNAs, researchers have reported that miRNAs are involved in the development of several cancer types [42]. In the present study, based on the genes in the prognostic model associated with mast cells-resting, 3 miRNA, including miR-145-5p, miR-29c-3p, and miR-335-3p, were predicted based on the databases (miRWalk3.0, TargetScan, MiRDB, and MirTarBase) with the Score > 0.95, and the miRNAs-TFs-mRNA co-regulation network was constructed. Among these target miRNAs, miR-29c-3p is reportedly down-regulated in meningioma [43], and Dalan et al [44] indicated that low expression of miR-29c-3p correlated significantly with higher recurrence rates in meningioma patients. However, no evidence of a correlation between hsa-miR-145-5p, or miR-335-3p and meningioma was reported till now. Notwithstanding, miR-145-5p is linked to psychiatric and neurodegenerative disorders [45]. Further, circPTN can sponge miR-145-5p to promote stemness or proliferation in glioma [46]. Hence, based on the findings, we speculate that the miRNAs, including miR-29c-3p and miR-145-5p associated with mast cells resting may cause meningioma.

Conclusions

In conclusion, this study conducted a bioinformatics analysis of DEGs related to mast cells resting, and deregulated pathways based on GSE43290, GSE77259 and GSE16581 datasets. DEGs of *MYC* and *CXCL8*, miRNAs of miR-29c-3p and miR-145-5p, as well as pathways such as the TNF signaling pathway, cytokine-cytokine receptor interaction, and IL-17 signaling pathway, probably involved in meningioma development, were obtained. These findings could improve the understanding of the pathogenesis and molecular mechanisms of mast cells resting in meningioma. Taken together, this was the first study to explore gene signatures related to mast cells resting in meningioma by a bioinformatics analysis. Moreover, this study combined immune infiltration with prognostic risk models in the meningioma direction; meanwhile, CIBERSORT deconvolution algorithm was used to quantify the infiltration abundance of each immune cell, and the correlation between modules and immune cells was calculated. However, further clinical studies are required to confirm the function of the identified genes.

Abbreviations

GEO: Gene Expression Omnibus; PPI: protein-protein interaction; Tregs: regulatory T cells; CNS: central nervous system; MCs: mast cells; TF: transcription factors; DEG: Differentially Expressed Gene; GO: Gene Ontology; KEGG: Kyoto Encyclopedia of Genes and Genomes; RMA: Robust Multiarray Average; PCA: principal component analysis; STRING: Search Tool for the Retrieval of Interacting Genes; DGIdb: Drug

Gene Interaction database; BP: Biological Process; CC: Cellular Component; MF: Molecular Function; TNF: Tumor Necrosis Factor.

Declarations

Acknowledgements

The authors thank all members in our lab for the excellent technical help.

Authors' contributions

WCL conceived and designed this study. HX carried out the plan and wrote this paper. XHD, CY, JJL and ZYL gave advice and carried out the data analysis. All authors read and approved the final manuscript.

Funding

This work was supported by grants from Guidance Plan of Natural Science Foundation of Liaoning Province (No. 201602773; 2019-ZD-0340) and Project of Science and Technology Plan of Liaoning Province (No. 20180550093).

Availability of data and material

Data sharing is not applicable to this article as no new data were created or analyzed in this study.

Ethics approval and consent to participate

This work was approved by the Ethical Board of China Medical University.

Consent of publication

Not applicable.

Competing interests

The authors declare that they have no competing interests.

Author details

¹ Department of Histology and Embryology, College of Basic Medicine, Shenyang Medical College, Shenyang, Liaoning, China

² Graduate Program in Bioinformatics and Computational Biology, University of Minnesota, Minneapolis, USA.

³ Department of Neurosurgery, General Hospital of Northern Theater Command, Shenyang, Liaoning, China

⁴ Department of Laboratory Animal Center, China Medical University, Shenyang, Liaoning, China

⁵ Department of Neurosurgery, First Affiliated Hospital of China Medical University, Shenyang, Liaoning, China

References

1. Ostrom QT, Gittleman H, Farah P, Ondracek A, Chen Y, Wolinsky Y, Stroup NE, Kruchko C, Barnholtz-Sloan JS. CBTRUS Statistical Report: Primary Brain and Central Nervous System Tumors Diagnosed in the United States in 2006-2010. *Neuro Oncology*, 15(suppl 2):ii1-ii56.
2. Rogers L, Barani I, Chamberlain M, Kaley TJ, McDermott M, Raizer J, Schiff D, Weber DC, Wen PY, Vogelbaum MA. Meningiomas: knowledge base, treatment outcomes, and uncertainties. A RANO review. *Journal of Neurosurgery*, 2015, 122(1):4-23.
3. Maxwell M, Galanopoulos T, Neville-Golden J, Antoniades HN. Expression of androgen and progesterone receptors in primary human meningiomas. *Journal of Neurosurgery*, 1993, 78(3):456-462.
4. Probst-Cousin S, Villagran-Lillo R, Lahl R, Bergmann M, Schmid KW, Gullotta F. Secretory meningioma: Clinical, histologic, and immunohistochemical findings in 31 cases. *Cancer*, 1997, 79(10):2003-2015.
5. Madhusoodanan S, Patel S, Reinhart J, Hines A, Serper M. Meningioma and psychiatric symptoms: A case report and brief review. *Annals of Clinical Psychiatry* 2015, 27(2):126-133.
6. El-Zein R, Bondy M, Wrensch M. Epidemiology of Brain Tumors; 2005.
7. Nakasu S, Fukami T, Jito J, Nozaki K. Recurrence and regrowth of benign meningiomas. *Brain Tumor Pathology*, 2009, 26(2):69-72.
8. Xiong Y, Kang W, He Z, Linglong P, Wenxian Y, Zhongxue F. Profiles of immune infiltration in colorectal cancer and their clinical significant: A gene expression-based study. *Cancer Medicine*. 2018;7(9):4496-4508.
9. Liu X, Wu S, Yang Y, Min Z, Hou Z. The prognostic landscape of tumor-infiltrating immune cell and immunomodulators in lung cancer. *Biomedicine & Pharmacotherapy* 2017, 95:55-61.
10. Jyothi, Thyagabhan, Mony, Matthew, Schuchert. Prognostic Implications of Heterogeneity in Intra-tumoral Immune Composition for Recurrence in Early Stage Lung Cancer. *Front Immunol*. 2018;9:2298.
11. Pagès F, Galon J, Dieu-Nosjean M-C, Tartour E, Sautès-Fridman C, Fridman W-H. Immune infiltration in human tumors: a prognostic factor that should not be ignored. *Oncogene*. 2010, 29(8):1093-1102.
12. Viel S, Charrier E, Marais A, Rouzaire P, Bienvenu J, Karlin L, Salles G, Walzer T. Monitoring NK cell activity in patients with hematological malignancies. *Oncoimmunology*, 2013, 2(9):e26011.
13. Stavros Polyzoidis, Triantafyllia Koletsas, Smaro Panagiotidou, Keyoumars Ashkan, Theoharis C Theoharides. Mast cells in meningiomas and brain inflammation. *Journal of Neuroinflammation*,

2015, 12(1):170.

14. Tirakotai W, Mennel HD, Celik I, Hellwig D, Bertalanffy H, Riegel T. Secretory meningioma: immunohistochemical findings and evaluation of mast cell infiltration. *Neurosurgical Review*, 2006, 29(1):41-48.
15. Gentleman RC, Carey VJ, Bates DM, et al. Bioconductor: open software development for computational biology and bioinformatics. *Genome biology*, 2004;5(10):R80.
16. Laurent G, Leslie C, Bolstad BM, Irizarry RA. affy—analysis of Affymetrix GeneChip data at the probe level. *Bioinformatics* 2004;20(3):3.
17. Smyth GK. limma: Linear Models for Microarray Data. 2011:397–420.
18. Aaron, Newman, Chih, Long, Liu, Michael, Green, Andrew. Robust enumeration of cell subsets from tissue expression profiles. *Nat Methods*. 2015;12(5):453-7.
19. Langfelder P, Horvath S. WGCNA: an R package for weighted correlation network analysis. *BMC Bioinformatics*. 2008, 9(1):559.
20. COX D. Regression models and life tables. *Journal of the Royal Statistical Society* 1972, 34.
21. Han H, Jae-Won C, Sangyoung L, Yun A, Hyojin K, Dasom B, Yang S, Yeong KC, Muyoung L, Eunbeen K. TRRUST v2: an expanded reference database of human and mouse transcriptional regulatory interactions. *Nucleic acids research* 2017(D1):D1.
22. Szklarczyk D, Morris JH, Cook H, Kuhn M, Wyder S, Simonovic M, Santos A, Doncheva NT, Roth A, Bork P. The STRING database in 2017: quality-controlled protein–protein association networks, made broadly accessible. *Nucleic acids research*, 2017, 45(D1):D362-D368.
23. Tang Y, Li M, Wang J, Pan Y, Wu FX. CytoNCA: A cytoscape plugin for centrality analysis and evaluation of protein interaction networks. *Biosystems*, 2015;127:67-72.
24. Bader GD, Hogue CW. An automated method for finding molecular complexes in large protein interaction networks. *BMC Bioinformatics*. 2003 ,13;4:2.
25. Cotto KC, Wagner AH, Yang-Yang F, Susanna K, Coffman AC, Gregory S, Alex W, Spies NC, Griffith OL, Malachi G. DGIdb 3.0: a redesign and expansion of the drug–gene interaction database. *Nucleic acids research* 2018 ,46(D1):D1068-D1073.
26. Vivian L, Craig K, Yannick D, Tim J, Guo AC, Liu Y, Adam M, David A, Michael W, Vanessa N. DrugBank 4.0: shedding new light on drug metabolism. *Nucleic acids research*. 2014;42:D1091-7.
27. Reszec J, Hermanowicz A, Rutkowski R,et al. Evaluation of mast cells and hypoxia inducible factor-1 expression in meningiomas of various grades in correlation with peritumoral brain edema. *J Neurooncol*. 2013, 115(1):119-125.
28. Sachpekidis C, Larribere L, Pan L, Haberkorn U, Dimitrakopoulou-Strauss A, Hassel JC. Predictive value of early 18F-FDG PET/CT studies for treatment response evaluation to ipilimumab in metastatic melanoma: preliminary results of an ongoing study. *European Journal of Nuclear Medicine & Molecular Imaging*, 2015, 42(3):386-396.

29. Butterfield LH. Recent advances in immunotherapy for hepatocellular cancer. *Swiss Medical Weekly*. 2007; 137(5-6):83-90.
30. Domingues PH, Teodósio C, Ortiz J, Sousa P, Otero á, Maillo A, Bárcena P, García-Macias MC, Lopes MC, de Oliveira C. Immunophenotypic Identification and Characterization of Tumor Cells and Infiltrating Cell Populations in Meningiomas. *American Journal of Pathology*, 2012, 181(5):1749-1761.
31. Herold-Mende C, Ull T, Rapp C, Dettling S, Jungk C, Sahm F, Von Deimling A, Unterberg A, Simon M. IMPS-14 PROGNOSTIC ROLE OF REGULATORY T-CELLS IN PRIMARY AND RECURRENT MENINGIOMA. *Neuro Oncology*, 2015, 17(suppl 5):v116.111-v116.
32. Gelerstein E, Berger A, Jonas-Kimchi T, Strauss I, Kanner AA, Blumenthal DT, Gottfried M, Margalit N, Ram Z, Shahar T. Regression of intracranial meningioma following treatment with nivolumab: Case report and review of the literature. *Journal of Clinical Neuroscience*, 37:51-53.
33. Dai J, Yanbin M, Shenghua C, Nanyang L, Jun C, Yang W. Identification of key genes and pathways in meningioma by bioinformatics analysis. *Oncology Letters*. 2018, 15(6):8245-8252.
34. Dong-Ling, Liu, Li-Xue, Zhao, Shuang, Zhang, Jun-Rong, Du. Peroxiredoxin 1-mediated activation of TLR4/NF-κB pathway contributes to neuroinflammatory injury in intracerebral hemorrhage. *Int Immunopharmacol*. 2016, 41:82-89.
35. Souza PS, Gonçalves ED, Pedroso GS, Farias HR, Junqueira SC, Marcon R, Tuon T, Cola M, Silveira PCL, Santos AR. Physical Exercise Attenuates Experimental Autoimmune Encephalomyelitis by Inhibiting Peripheral Immune Response and Blood-Brain Barrier Disruption. *Molecular Neurobiology*. 2017, 54(6):4723-4737.
36. Gelderblom M, Weymar A, Bernreuther C, Velden J, Magnus T. Neutralization of the IL-17 axis diminishes neutrophil invasion and protects from ischemic stroke. *Blood*. 2012, 120(18):3793-3802.
37. Jennifer K. Grenier PAF, Erica A. Sloma, Andrew D. Miller. RNA-seq transcriptome analysis of formalin fixed, paraffin-embedded canine meningioma. *PloS one*. 2017, 12(10).
38. Cai Z, Zou Y, Hu H, Lu C, Hu G. RIZ1 negatively regulates ubiquitin-conjugating enzyme E2C/UbcH10 via targeting c-Myc in meningioma. *American Journal of Translational Research*. 2017, 9(5):2645-2655.
39. Ren, Xiaohui, Wu, Zhen, Zhang, Junting, Hao, Shuyu, Bi, Zhiyong. Methylation of Werner syndrome protein is associated with the occurrence and development of invasive meningioma via the regulation of Myc and p53 expression. *Exp Ther Med*. 2015, 10(2):498-502.
40. BARBIERI F, BAJETTO A, PORCILE C, PATTAROZZI A, MASSA A, LUNARDI G, ZONA G, DORCARATTO A, RAVETTI JL, SPAZIANTE R. CXC Receptor and Chemokine Expression in Human Meningioma: SDF1/CXCR4 Signaling Activates ERK1/2 and Stimulates Meningioma Cell Proliferation. *Annals of the New York Academy of Sciences*. 2006, 1090:332-343 .
41. Wu X-J, Zhou X-B, Chen C, Mao W. Systematic Investigation of Quercetin for Treating Cardiovascular Disease Based on Network Pharmacology. *Combinatorial Chemistry & High Throughput Screening*. 2019, 22(6):411-420.

42. Klinge, Carolyn M. Noncoding RNAs: long non-coding RNAs and microRNAs in endocrine-related cancers. *Endocrine Related Cancer*. 2018, 25(4):R259-R282.
43. Galania V, Lamprib E, Varouktsic A, Alexioud G, Mitselou A. Genetic and epigenetic alterations in meningiomas. *Clinical Neurology & Neurosurgery* 2017, 158:119-125.
44. Zhi F, Zhou G, Wang S, Shi Y, Yang Y. A microRNA expression signature predicts meningioma recurrence. *International Journal of Cancer*. 2013, 132(1):128-136.
45. HA W, D K, S W, H S, SL S, C B, M S-M, DS D, DS P, H L et al. MicroRNA sequencing of rat hippocampus and human biofluids identifies acute, chronic, focal and diffuse traumatic brain injuries. *Scientific reports* 2020, 10(1):3341.
46. J C, T C, Y Z, Y L, Y Z, Y W, X L, X X, J W, M H et al. circPTN sponges miR-145-5p/miR-330-5p to promote proliferation and stemness in glioma. *Journal of experimental & clinical cancer research*. 2019, 38(1):398.

Tables

Table 1 The univariate and multivariate Cox regression analysis

Gene	Univariate analysis				Multivariate analysis			
	HR	lower.95	upper.95	p.val	HR	lower.95	upper.95	p.val
CXCL8	1.002	1.001	1.004	0.001	1.007	1.001	1.014	0.025
MYC	1.002	1.001	1.004	0.003	1.003	1.000	1.005	0.030
CXCL2	1.010	1.003	1.017	0.006				
CXCL3	1.007	1.002	1.013	0.008				
TNFAIP3	1.002	1.001	1.004	0.010				
FOSL1	1.031	1.002	1.061	0.036				
HIST1H2BN	1.147	1.008	1.305	0.038				
BCL2A1	1.007	1.000	1.014	0.038				
SLC2A3	1.001	1.00	1.002	0.0495				

Figures

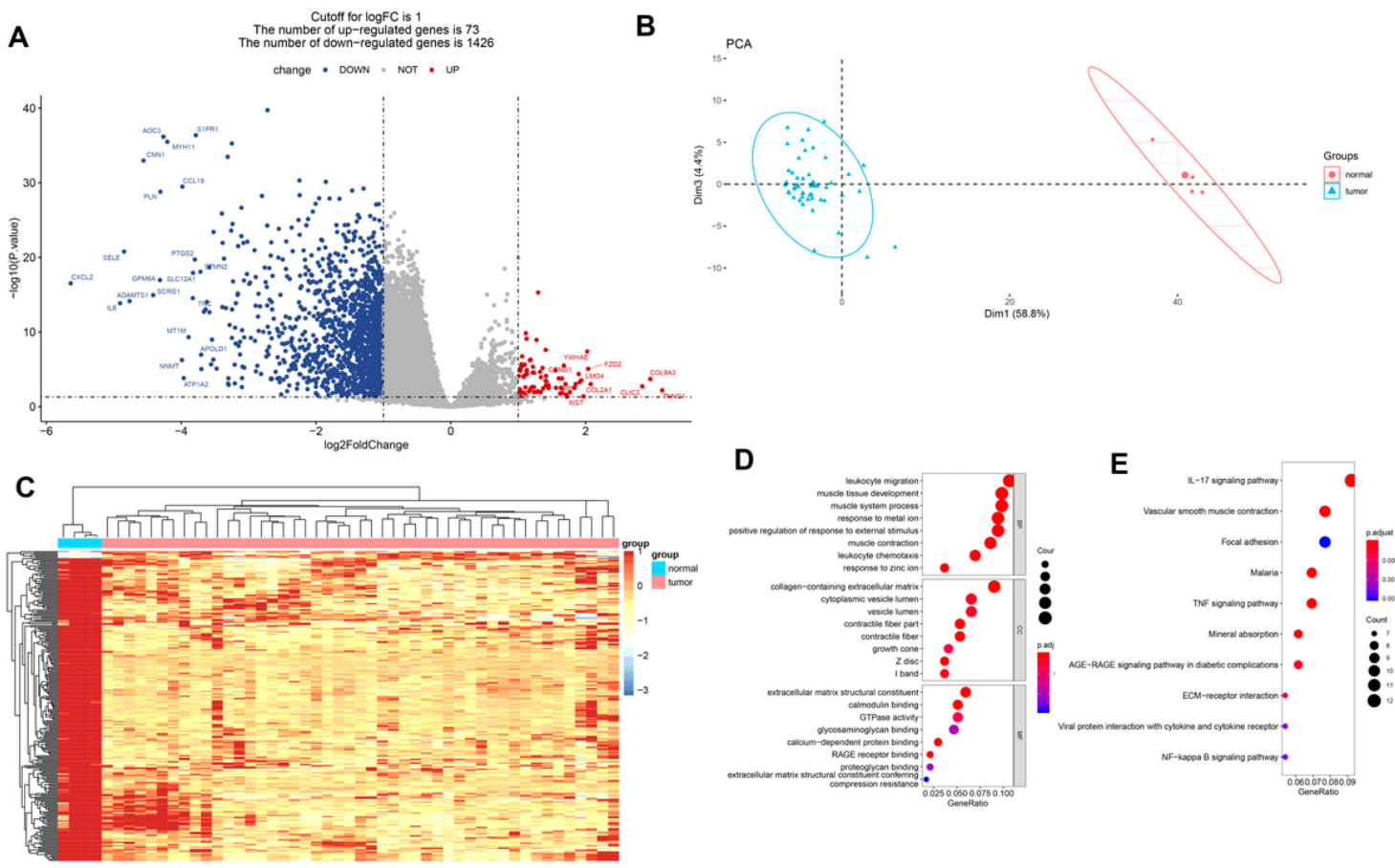


Figure 1

Clustering analysis. Volcano plot (A), PCA clustering (B) and bilayer Heat map clustering (C) exhibit the differentially expressed DEGs between the two groups could be significantly distinguished.

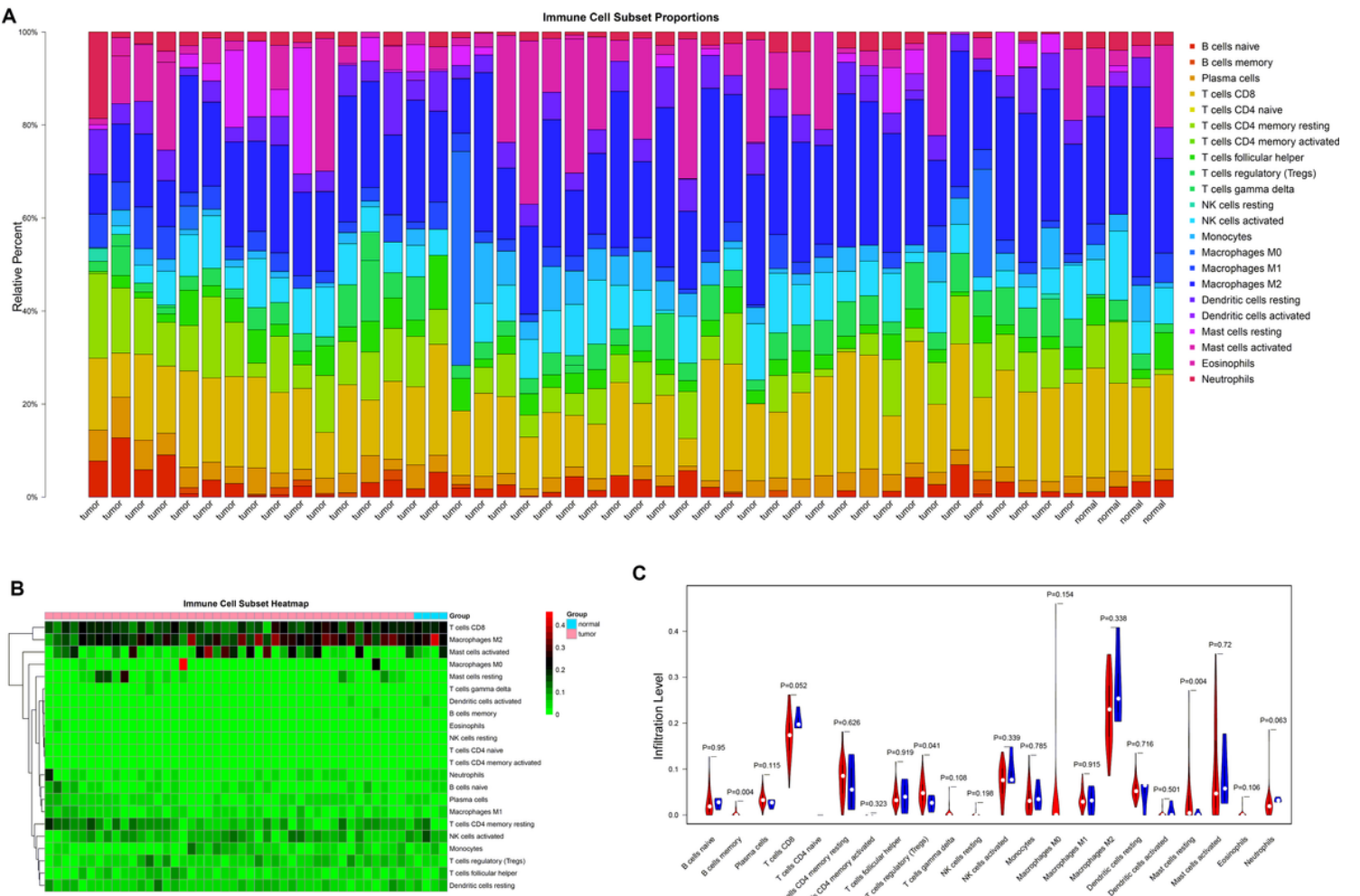


Figure 2

The landscape of immune infiltration in meningiomas cohort. (A) The difference of 22 immune infiltration between the meningiomas and control groups; (B) Heatmap of the 22 immune cell proportions; (C) The violin plot. Red represents tumor group, and blue represents the normal group.

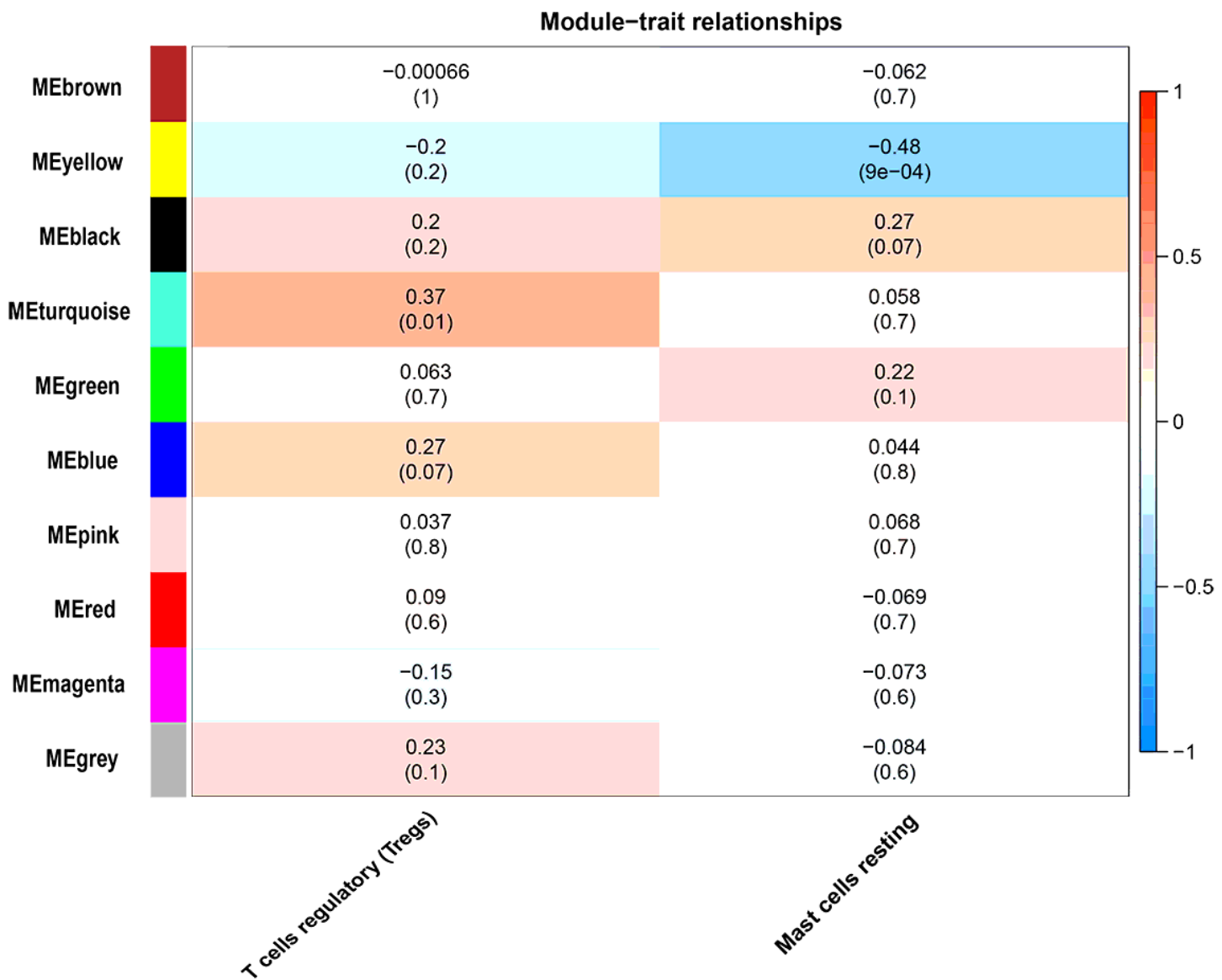


Figure 3

Heatmap between each module and the degree of invasion of immune cells in tumor tissue.

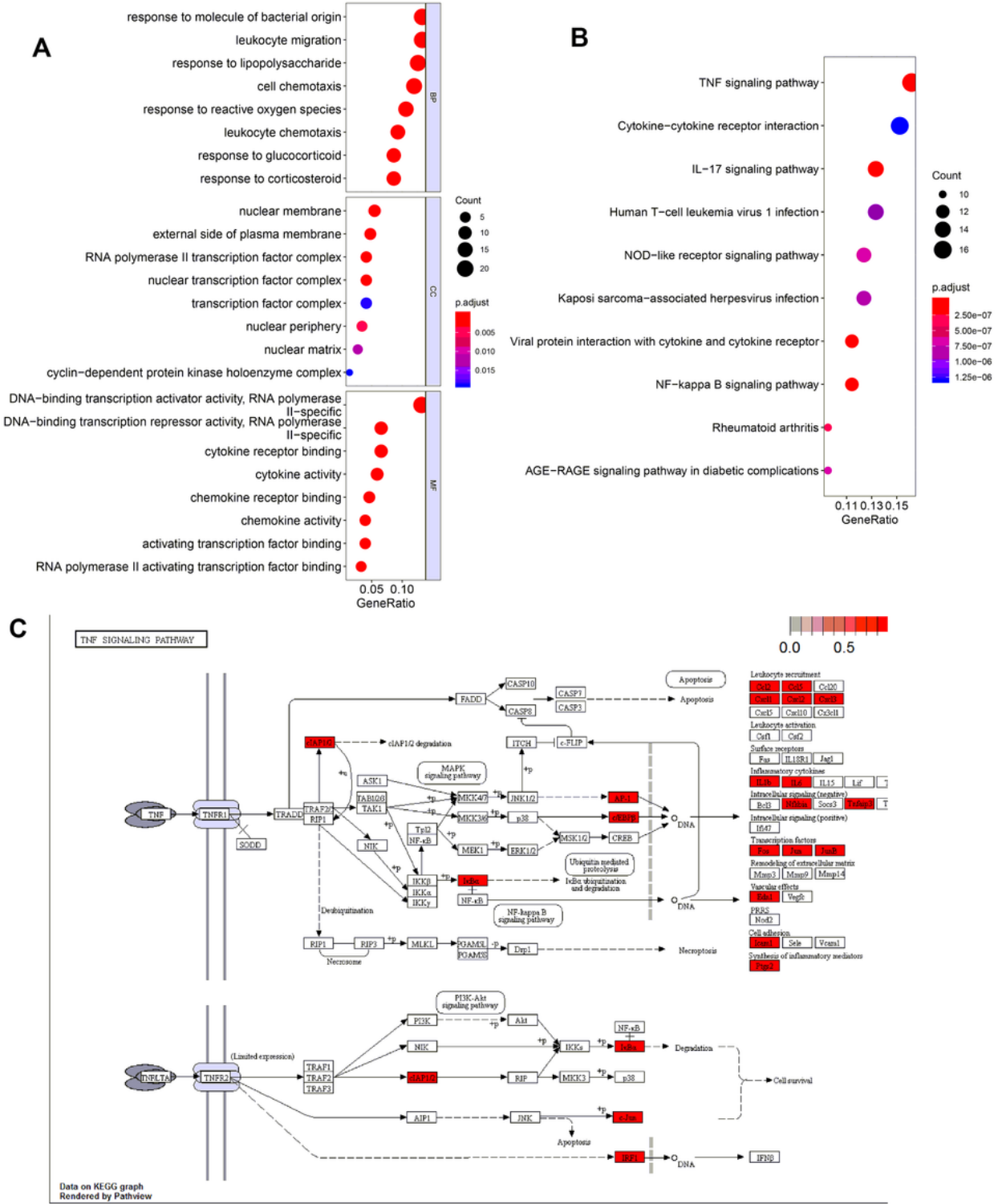


Figure 4

Functional analysis of differential expression genes related to resting mast cells infiltration. (A) Gene Ontology annotations consists of biological processes. (B) Kyoto Encyclopedia of Genes and Genomes pathway. (C) The path diagram of IL-17 signaling pathway.

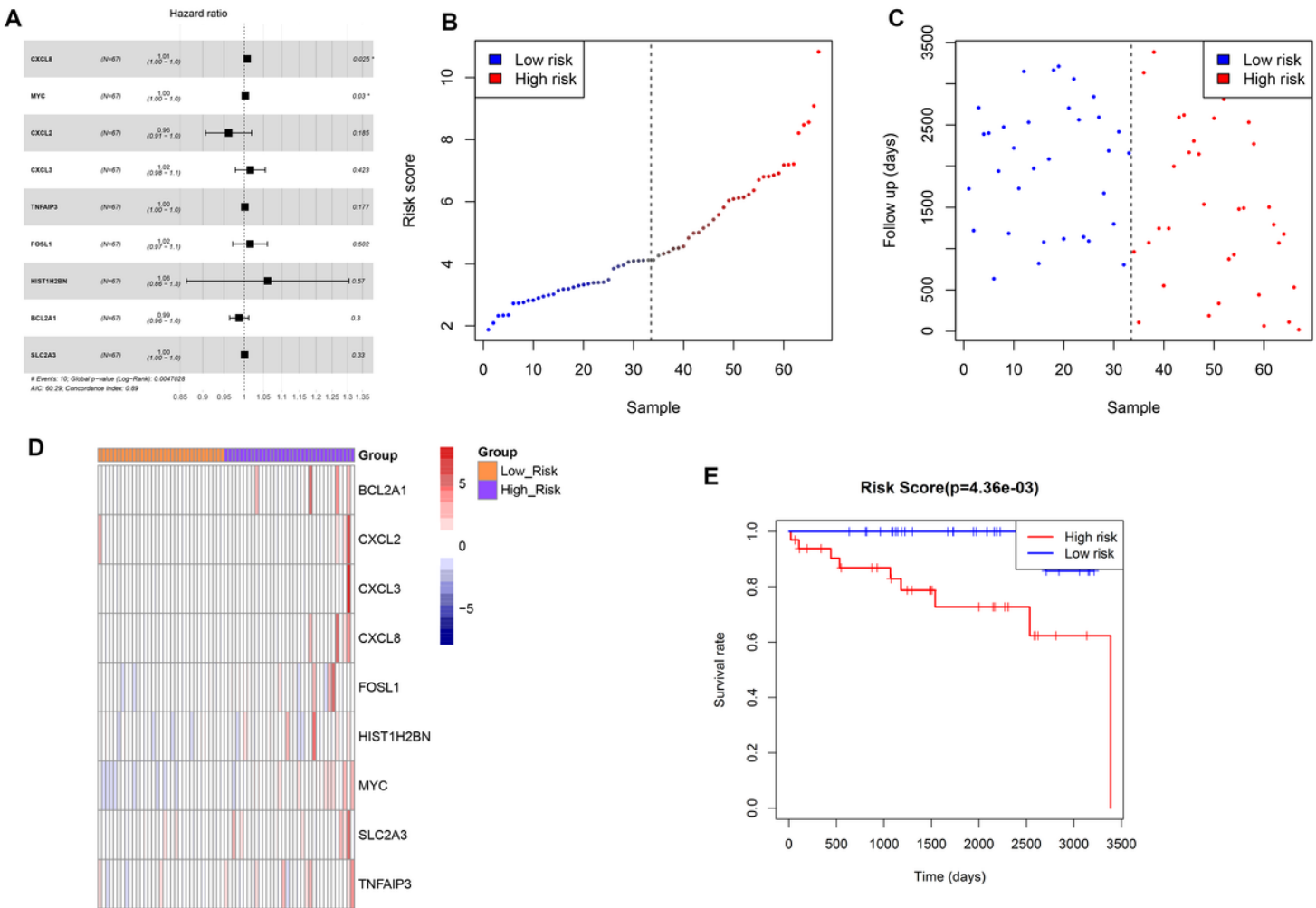


Figure 5

Survival analysis. (A) HR's forest map of Cox multivariate analysis. (B) The classification curve of the sample risk model. (C) Survival time scatter plot of risk model. (D) Clustering heat map of genes in a risk model. (E) The K-M survival curve of the risk model.

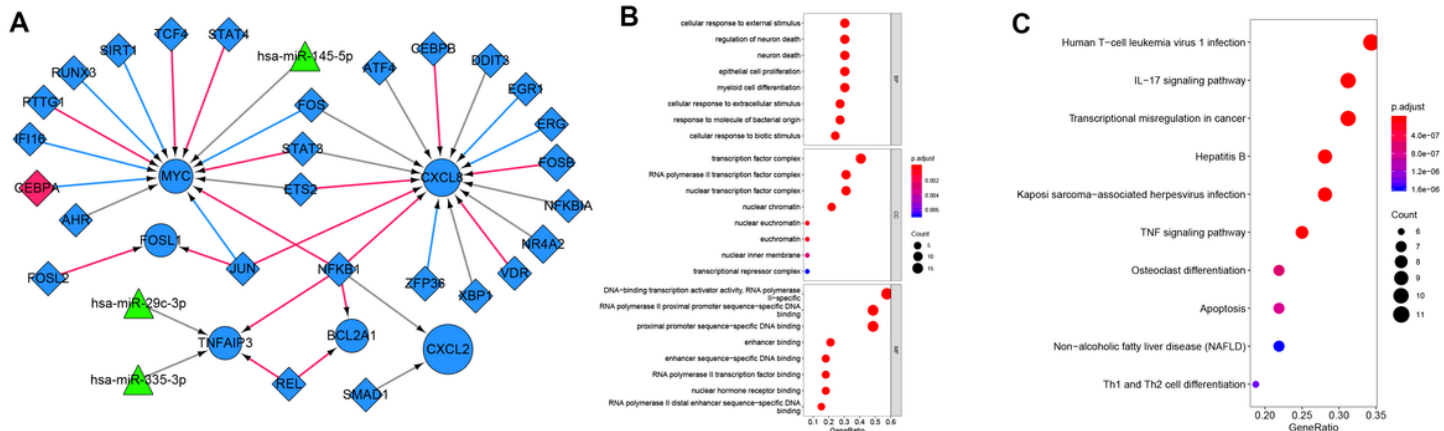


Figure 6

The miRNA-transcription factor (TF)-mRNA regulatory network (A) and enrichment analysis (B).

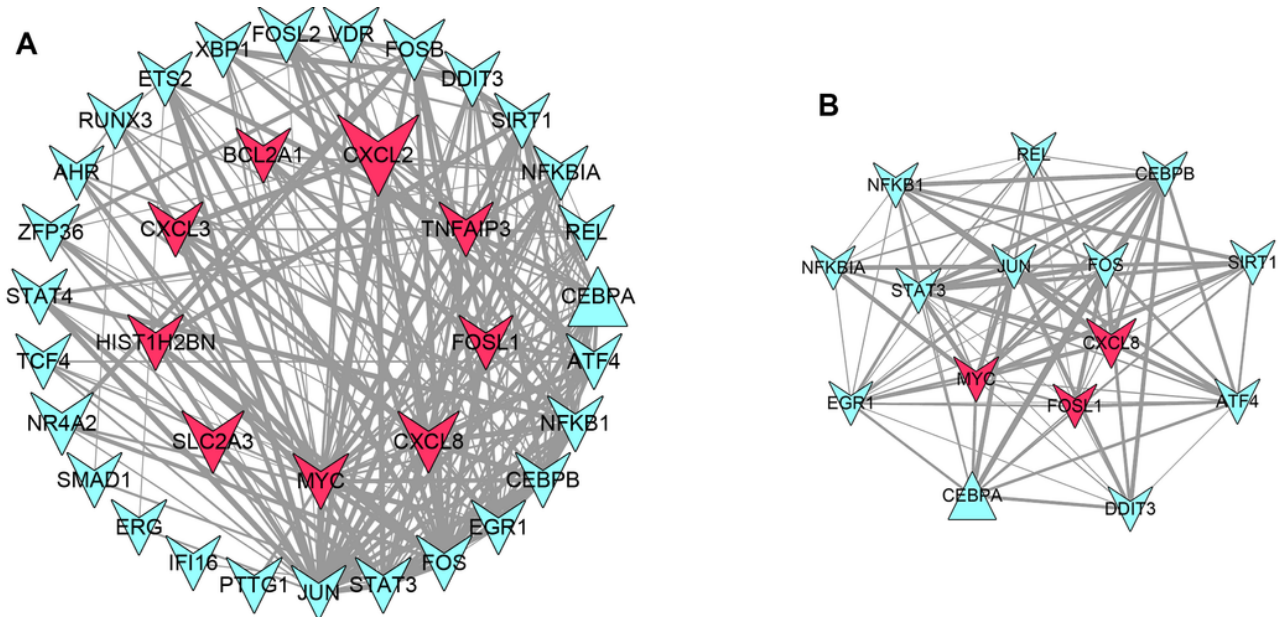


Figure 7

The protein-protein interaction (PPI) network and modules analysis. (A) The PPI network. (B) The module network. The triangle node represents up-regulated differential gene; Arrowhead nodes represent down-regulated differential genes; The red nodes represent the differential genes in the prognostic model, and the blue nodes represent other differential genes.

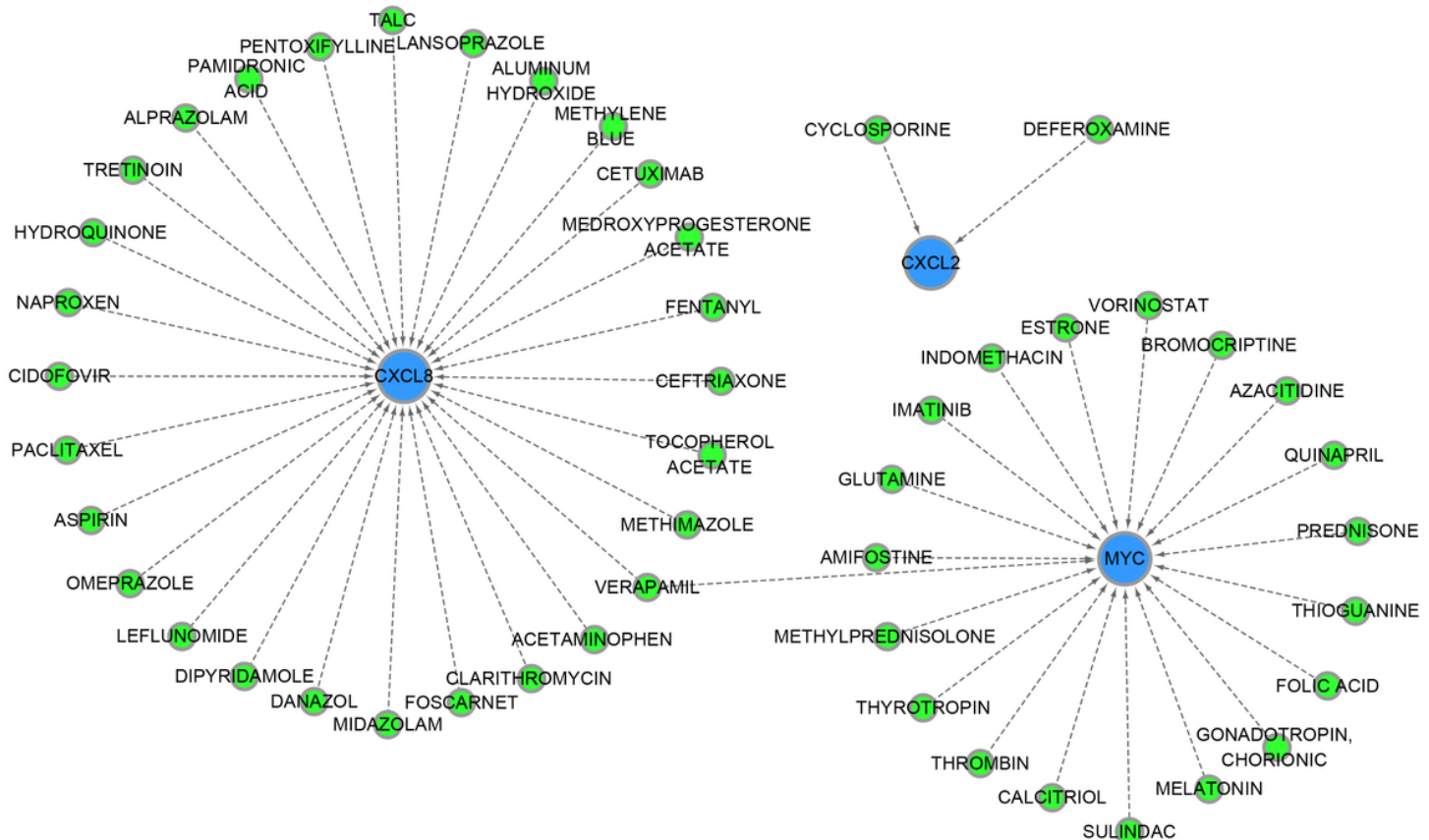


Figure 8

Drug-gene network. Blue represents downregulated genes in prognostic risk model, and green represents drugs, respectively.

Supplementary Files

This is a list of supplementary files associated with this preprint. Click to download.

- [Supplementaryfigure1.tif](#)
- [Supplementaryfigure2.tif](#)
- [Supplementarytable1.xlsx](#)
- [Supplementarytable2.xlsx](#)